# Detection of Majorana fermions in an Aharonov–Bohm interferometer*

Shang En-Ming(尚恩明)†, Pan Yi-Ming(潘义明), Shao Lu-Bing(邵陆兵), and Wang Bai-Gen(王伯根)

*National Laboratory of Solid State Microstructures and School of Physics, Nanjing University, Nanjing* 210093, *China*

(Received 17 August 2013; revised manuscript received 21 October 2013; published online 25 March 2014)

By using the non-equilibrium Green's function technique, we investigate the electronic transport properties in an Aharonov–Bohm interferometer coupling with Majorana fermions. We find a fixed unit conductance peak which is independent of the other factors when the topological superconductor is grounded. Especially, an additional phase appears when the topological superconductor is in the strong Coulomb regime, which induces a new conductance resonant peak compared with the structure of replacing the topological superconductor by a quantum dot, and the conductance oscillation with the magnetic flux reveals a $2\pi$ phase shift by raising (lowering) a charge on the capacitor.

**Keywords:** Majorana fermion, quantum dot, Aharonov–Bohm interferometer, Coulomb blockade

**PACS:** 72.10.Fk, 73.63.–b, 85.75.–d **DOI:** 10.1088/1674-1056/23/5/057201

## 1. Introduction

Recently, the search for the Majorana fermion (MF), whose anti-particle is itself,[1–4] has drawn a great deal of attention because the MF exhibits nonlocal features, such as teleportation and non-Abelian statistics.[5,6] The nonlocal property leads to interesting studies in quantum computation.[7] Some studies reveal that Majorana bound states (MBSs) can be realized at the ends of one-dimensional spinless p-wave superconductors[8–10] and the $5/2$ fractional quantum Hall system.[11] Interestingly, MBSs may also appear in a semiconductor with strong spin–orbit coupling or in a topological insulator,[12–14] proximity-induced superconductivity by putting on the surface of an s-wave superconductor.[15–17] Two spatially separated MBSs can define a nonlocal zero-energy fermion level,[18] which can couple to other degrees of freedom. Therefore, it is possible to detect and verify the signature of MBSs in such materials by coupling to the normal materials.

An important challenge is the full experimental demonstration of the MFs in solid states. The electronic transport through the topological materials is one method to detect the features of the topological edge state.[19–21] MBSs are expected to produce a characteristic zero-voltage anomaly peak in the tunneling conductance.[9,12,22] Recently, this evidence for MF has been reported by Mourik *et al.*[23] and other groups in tunneling spectroscopy experiments using InSb or InAs nanowires.[24–26] However, this evidence is still debated.[27] Fu[28] proposed the teleportation via MBSs with a topological superconductor (TS) nanowire which is grounded by a capacitor in the strong Coulomb regime. The teleportation indicates that electron tunneling in and out of two separated MBSs is equivalent to the resonant tunneling through a single level quantum dot (QD) in the Coulomb blocked regime. However, little attention has been paid to an additional $\pi/2$ phase in the teleportation. This phase does not work in direct transmission, while in a path interference such as an Ahanorov–Bohm (AB) interferometer, the additional phase is significant in electronic transportation. It makes the teleportation via MBSs different from the transportation via a single level QD and gives rise to some new features in transportation.

Motivated by this additional phase and for finding the new signature of MFs, we apply the non-equilibrium Green function (NEGF) technique to investigate the charge transportation in an AB interferometer consisting of two parallel QDs and a TS nanowire. Here, we consider two special cases. (1) Without charging energy on the TS nanowire when it is grounded directly. In this case, we find a robust fixed conductance peak that is independent of other system parameters. (2) With strong charging energy on the TS nanowire when it is grounded via a capacitor, which indicates the electrons of the TS nanowire are in the strong Coulomb regime, a teleportation process occurs in this regime.[28] A new conductance peak outgrows between two fundamental resonant energies because of the additional $\pi/2$ phase. Moreover, the conductance oscillation reveals the period of $4\pi$ and has a $2\pi$ phase shift by changing the charging number of the capacitor on the asymmetrical coupling condition. These abnormal features suggest the existence of MFs.

*Project supported by the National Basic Research Program of China (Grant No. 2011CB922103).

†Corresponding author. E-mail: shangjin0491@163.com

© 2014 Chinese Physical Society and IOP Publishing Ltd 

## 2. Model and method

### 2.1. Model

The setup is shown in Fig. 1. An AB interferometer contains two QDs coupled to two ends of a semiconductor nanowire with strong Rashba spin–orbit interaction. The nanowire has proximity-induced superconductivity by putting it on the surface of an s-wave superconductor, and a strong magnetic field is applied along its axis (for simplicity, the s-wave superconductor and the magnetic field along the axis of the nanowire are not shown in Fig. 1). The spinless consideration is provided due to the spin–orbital coupling and the strong Zeeman splitting. Because of the proximity effect of the s-wave superconductor, the nontrivial superconductor phase resembles the p+ip superconductor phase, which has two separated MBSs at the two ends of the nanowire.[15–17] The nanowire is grounded via a capacitor with charging energy $E_c = e^2/2C$, where $C$ is the capacity. The two QDs attach two normal metallic reservoirs on the left and the right sides, a magnetic flux $\Phi$ threads into the whole AB ring (the ellipse as shown in Fig. 1). The model Hamiltonian can be written as

$$H = H_s + H_l + H_t + H_c, \tag{1a}$$

with

$$\begin{aligned} H_s &= H_0 + H_{Md} \\ &= \sum_i \varepsilon_i d_i^\dagger d_i + i\xi\gamma_1\gamma_2 + \sum_i \lambda_i (d_i - d_i^\dagger)\gamma_i, \end{aligned} \tag{1b}$$

$$H_l = \sum_{k,\eta} \varepsilon_{\eta k} c_{\eta k}^\dagger c_{\eta k}, \tag{1c}$$

$$H_t = \sum_{k,\eta}\sum_i (T_{i\eta} c_{\eta k}^\dagger d_i + \text{h.c.}), \tag{1d}$$

$$H_c = E_c(2N + n_d - n_0)^2, \tag{1e}$$

where the central system Hamiltonian $H_s$ includes the decoupled part $H_0$ and the interactive part $H_{Md}$; $H_0$ contains the Hamiltonian of the individual $i$-th QD with tunable energy level $\varepsilon_i$ and the coupling of two MBSs $\gamma_{1,2}$ which satisfy $\gamma_{1,2} = \gamma_{1,2}^\dagger$; and $d_i$ is the annihilation operator for electron in the $i$-th QD ($i = 1, 2$). The coupling coefficient $\xi$ depends on the length of the nanowire. The interactive part $H_{Md}$ describes the two QDs coupled to the two MBSs with tunneling amplitude $\lambda_i$. The $H_l$ is the Hamiltonian of the $\eta$ ($\eta = L, R$) leads of electron energy $\varepsilon_{\eta k}$ with momentum $k$, where $c_{\eta k}$ is the annihilation operator for electrons in the $\eta$ lead. The $H_t$ is the standard tunneling Hamiltonian between leads and QDs, where $(T_{1L})^* = (T_{1R}) = (T_{2L}) = (T_{2R})^* = |T|e^{\frac{i\varphi}{4}}$ with $\varphi = 2\pi\Phi/\Phi_0$, and $\Phi_0 = h/e$ is the flux quantum. Since the magnetic flux goes through the center of the AB ring, there is no phase difference due to the magnetic flux crossing the nanowire. The $H_c$ is an additional term due to the finite charging energy $E_c$,[28,29] where $N$ is the number of Cooper pairs in the superconductor, and $n_d = f^\dagger f$ satisfies $2i\gamma_1\gamma_2 = 2n_d - 1 = (-1)^{2N+1}$. The $n_0$ can be tuned by gate voltage $V_g$ across the capacitor.

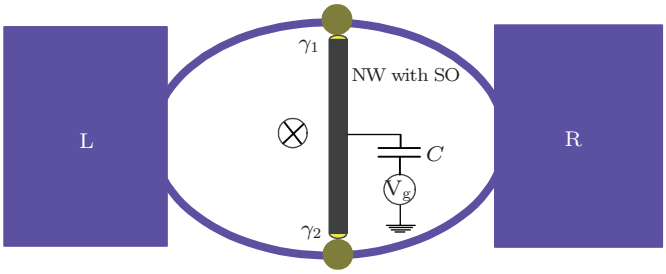



**Fig. 1.** (color online) The schematic diagram of a parallel double QD system connected to two normal metal leads. Between the two QDs, a semiconductor nanowire is placed on an s-wave superconductor surface with a strong magnetic field applied along the axis of the nanowire. Two MBSs labeled by $\gamma_1$ and $\gamma_2$ are located at the two ends of the nanowire, which are grounded indirectly via a capacitor with capacity $C$. The two QDs are coupled to MBSs by connecting them to the two ends of the nanowire. A magnetic flux $\Phi$ goes through the whole AB interferometer ring.

The current through the left lead can be calculated from the evolution of the electron number operator, $N_L = \sum_k c_{Lk}^\dagger c_{Lk}$. Setting the bias of the left (right) lead at $V_L$ ($V_R$) and applying the NEGF method, we obtain the current expression

$$\begin{aligned} I_L &= -e\langle \dot{N}_L \rangle \\ &= -\frac{e}{h}\int \frac{d\omega}{2\pi} \text{Tr}[(\boldsymbol{G}^r - \boldsymbol{G}^a)\boldsymbol{\Sigma}_L^< + (\boldsymbol{\Sigma}_L^a - \boldsymbol{\Sigma}_R^r)\boldsymbol{G}^<], \end{aligned} \tag{2}$$

where $\boldsymbol{G}^r(\omega)$ is defined as the Fourier-transformed retarded double time NEGF $G^r(t,t') = -i\theta(t-t')\langle\{\Psi(t), \Psi^\dagger(t')\}\rangle$,

$$\boldsymbol{G}^r(\omega) = [\omega\boldsymbol{I} - \boldsymbol{H}_s - \boldsymbol{\Sigma}^r(\omega)]^{-1}, \tag{3}$$

here $\Psi$ is the column vector of the central system, $\boldsymbol{I}$ represents the identity matrix, $\boldsymbol{H}_s$ is the Hamiltonian of the central system, and $\boldsymbol{\Sigma}^{r,a,<}(\omega) = \boldsymbol{\Sigma}_L^{r,a,<}(\omega) + \boldsymbol{\Sigma}_R^{r,a,<}(\omega)$ represent the retarded, the advanced, and the lesser self-energies of the system due to coupling with the leads. We can use the Keldysh equation to obtain the lesser NEGF, $\boldsymbol{G}^<(\omega) = \boldsymbol{G}^r(\omega)\boldsymbol{\Sigma}^<(\omega)\boldsymbol{G}^a(\omega)$, with $\boldsymbol{G}^a(\omega) = [\boldsymbol{G}^r(\omega)]^\dagger$. Under the wide-band approximation, the self-energies can be derived as

$$\boldsymbol{\Sigma}_\eta^{r,a}(\omega) = \mp\frac{i}{2}\boldsymbol{\Gamma}_\eta, \tag{4a}$$

$$\boldsymbol{\Sigma}_\eta^<(\omega) = i\boldsymbol{F}_\eta\boldsymbol{\Gamma}_\eta, \tag{4b}$$

where $\boldsymbol{F}_\eta$ is the about matrix form of the Fermi distribute function in the $\eta$ lead, and it has different forms in different bases. The $\boldsymbol{\Gamma}_\eta$ is the coupling matrix of the $\eta$ lead and the two QDs. The elements are $\Gamma_{ij}^\eta = 2\pi T_{i\eta}^* T_{j\eta}\rho_\eta$ with $\rho_\eta$ being the density of state of the $\eta$ lead, therefore $\Gamma_{12}^\eta = \sqrt{\Gamma_1^\eta\Gamma_2^\eta}$. In our work, we assume that $\rho_\eta$ is independent of energy, i.e., $\Gamma_{ij}^\eta$ are regarded as constants.

### 2.2. Two special cases

We consider two special cases: one without charging energy on the TS nanowire, i.e., the TS nanowire is grounded directly, and one with strong charging energy on the TS nanowire achieved by grounded via a capacitor. The two special cases will be discussed respectively.

#### 2.2.1. Without charging energy

When the TS nanowire is grounded directly, there is no charging energy on the TS nanowire. Actually, $H_{\rm Md}$ should include a condensate phase $\phi$ of the superconductor for raising or lowing the number of Cooper pairs. However, for the TS nanowire being grounded directly, the capacity $C\to\infty$ and $H_{\rm c}=0$, the phase can be absorbed in the operator of the QDs and MFs by using a BCS wave function.[30] Thus, it is convenient to convert the MFs to the regular fermion representation by $\gamma_1=\frac{1}{\sqrt{2}}(a+a^\dagger)$ and $\gamma_2=-{\rm i}\frac{1}{\sqrt{2}}(a-a^\dagger)$. The two parts of the central system Hamiltonian read

$$H_0=\sum_{i=1,2}\varepsilon_i d_i^\dagger d_i+\xi(a^\dagger a-1/2), \tag{5a}$$

$$H_{\rm Md}=\frac{\lambda_1}{\sqrt{2}}(d_1-d_1^\dagger)(a+a^\dagger)-\frac{{\rm i}\lambda_2}{\sqrt{2}}(d_2-d_2^\dagger)(a-a^\dagger). \tag{5b}$$

We use the basis $\boldsymbol{\Psi}=(d_1,d_1^\dagger,d_2,d_2^\dagger,a,a^\dagger)^{\rm T}$ to form the NEGF. The matrix form of the central system Hamiltonian and the coupling matrix are described as

$$\boldsymbol{H}_{\rm s}=\begin{bmatrix}
\varepsilon_1 & 0 & 0 & 0 & \frac{-\lambda_1}{\sqrt{2}} & \frac{-\lambda_1}{\sqrt{2}}\\
0 & -\varepsilon_1 & 0 & 0 & \frac{\lambda_1}{\sqrt{2}} & \frac{\lambda_1}{\sqrt{2}}\\
0 & 0 & \varepsilon_2 & 0 & \frac{{\rm i}\lambda_2}{\sqrt{2}} & \frac{-{\rm i}\lambda_2}{\sqrt{2}}\\
0 & 0 & 0 & -\varepsilon_2 & \frac{-{\rm i}\lambda_2}{\sqrt{2}} & \frac{{\rm i}\lambda_2}{\sqrt{2}}\\
\frac{-\lambda_1}{\sqrt{2}} & \frac{\lambda_1}{\sqrt{2}} & \frac{-{\rm i}\lambda_2}{\sqrt{2}} & \frac{{\rm i}\lambda_2}{\sqrt{2}} & \xi & 0\\
\frac{-\lambda_1}{\sqrt{2}} & \frac{\lambda_1}{\sqrt{2}} & \frac{{\rm i}\lambda_2}{\sqrt{2}} & \frac{-{\rm i}\lambda_2}{\sqrt{2}} & 0 & -\xi
\end{bmatrix}, \tag{6}$$

$$\boldsymbol{\Gamma}_{\rm L/R}=\begin{bmatrix}
\Gamma_1^{\rm L/R} & 0 & \Gamma_{12}^{\rm L/R}{\rm e}^{\mp\frac{{\rm i}\varphi}{2}} & 0 & 0 & 0\\
0 & \Gamma_1^{\rm L/R} & 0 & \Gamma_{12}^{\rm L/R}{\rm e}^{\pm\frac{{\rm i}\varphi}{2}} & 0 & 0\\
\Gamma_{12}^{\rm L/R}{\rm e}^{\pm\frac{{\rm i}\varphi}{2}} & 0 & \Gamma_2^{\rm L/R} & 0 & 0 & 0\\
0 & \Gamma_{12}^{\rm L/R}{\rm e}^{\mp\frac{{\rm i}\varphi}{2}} & 0 & \Gamma_2^{\rm L/R} & 0 & 0\\
0 & 0 & 0 & 0 & 0 & 0\\
0 & 0 & 0 & 0 & 0 & 0
\end{bmatrix}. \tag{7}$$

Note that the sign of exponent in $\boldsymbol{\Gamma}_{\rm L/R}$ takes the first sign for $\eta={\rm L}$ and the second sign for $\eta={\rm R}$. The matrix form of the Fermi distribution function in this basis is $\boldsymbol{F}_\eta=\begin{bmatrix} f_-^\eta & 0\\ 0 & f_+^\eta\end{bmatrix}\otimes\boldsymbol{I}_{3\times3}$, where $f_\pm^\eta=f(\omega\pm eV_\eta)$ represents the electron (positive sign) or hole (minus sign) Fermi distribution function of the $\eta$ lead.

By using the Keldysh equation and the identity $\boldsymbol{G}^{\rm r}-\boldsymbol{G}^{\rm a}=\boldsymbol{G}^{\rm r}(\boldsymbol{\Sigma}^{\rm r}-\boldsymbol{\Sigma}^{\rm a})\boldsymbol{G}^{\rm a}$, Eq. (2) can be rewritten explicitly as

$$\begin{aligned}I_{\rm L}=&-\frac{e}{h}\int\frac{{\rm d}\omega}{2\pi}[T_1(f_-^{\rm L}-f_+^{\rm L})+T_2(f_-^{\rm L}-f_+^{\rm R})\\&+T_3(f_-^{\rm L}-f_-^{\rm R})],\end{aligned} \tag{8}$$

with

$$\begin{aligned}T_1=&\,\Gamma_{\rm L}^2\Bigg(\sum_{i=1,3}\sum_{j=2,4}|G_{ij}^{\rm r}|^2+2{\rm Re}[G_{32}^{\rm r}G_{41}^{\rm a}+G_{12}^{\rm r}G_{43}^{\rm a}{\rm e}^{{\rm i}\varphi}\\&+(G_{12}^{\rm r}G_{41}^{\rm a}+G_{12}^{\rm r}G_{23}^{\rm a}+G_{14}^{\rm r}G_{43}^{\rm a}+G_{32}^{\rm r}G_{43}^{\rm a}){\rm e}^{\frac{{\rm i}\varphi}{2}}]\Bigg),\end{aligned} \tag{9a}$$

$$\begin{aligned}T_2=&\,\Gamma_{\rm L}\Gamma_{\rm R}(\sum_{i=1,3}\sum_{j=2,4}|G_{ij}^{\rm r}|^2+2{\rm Re}[G_{12}^{\rm r}G_{43}^{\rm a}+G_{14}^{\rm r}G_{23}^{\rm a}{\rm e}^{{\rm i}\varphi}\\&+(G_{12}^{\rm r}G_{23}^{\rm a}+G_{14}^{\rm r}G_{43}^{\rm a}+G_{34}^{\rm r}G_{23}^{\rm a}+G_{14}^{\rm r}G_{21}^{\rm a}){\rm e}^{\frac{{\rm i}\varphi}{2}}]),\end{aligned} \tag{9b}$$

$$\begin{aligned}T_3=&\,\Gamma_{\rm L}\Gamma_{\rm R}(\sum_{i,j=1,3}|G_{ij}^{\rm r}|^2+2{\rm Re}[G_{13}^{\rm r}G_{13}^{\rm a}+G_{11}^{\rm r}G_{33}^{\rm a}{\rm e}^{{\rm i}\varphi}\\&+(G_{11}^{\rm r}G_{31}^{\rm a}+G_{11}^{\rm r}G_{13}^{\rm a}+G_{13}^{\rm r}G_{33}^{\rm a}+G_{31}^{\rm r}G_{33}^{\rm a}){\rm e}^{\frac{{\rm i}\varphi}{2}}]).\end{aligned} \tag{9c}$$

At a low temperature, the linear conductance can be obtained by $G=\frac{\partial I}{\partial V}|_{V\to0}$, where $V=|V_{\rm L}-V_{\rm R}|$ is the voltage drop between the two leads,

$$G=\frac{e^2}{h}(2T_1+T_2+T_3). \tag{10}$$

The physical meaning of the above equation is clear. Here $T_1$ represents the coefficient of the local Andreev reflection (AR), i.e., an electron transport from the left lead into the central system and a hole is reflected back; $T_2$ represents the coefficient of the cross AR or non-local AR, i.e., an electron transport from the left (right) lead and a hole is reflected at the right (left) lead; $T_3$ is the transmission coefficient of single electronic tunneling.

#### 2.2.2. With strong charging energy

In the case of the nanowire grounded via a capacitor and so with strong charging energy, we consider the low-energy spectrum with $\omega\ll E_{\rm c}$, which are both lower than the superconductor gap. In the strong Coulomb regime, the charging energy is dominant, the phase of the superconductor $\phi$ for raising or lowering the number of Cooper pairs must be considered. Therefore, $H_{\rm Md}$ should be in the form of

$$H_{\rm Md}=\frac{\lambda_1}{\sqrt{2}}d_1^\dagger(a+{\rm e}^{-{\rm i}\phi}a^\dagger)-\frac{{\rm i}\lambda_2}{\sqrt{2}}d_2^\dagger(a-{\rm e}^{-{\rm i}\phi}a^\dagger)+{\rm h.c.}, \tag{11}$$

which means that the charge is conserved.

Furthermore, in the strong Coulomb regime, the resonant situation for the central system is determined by two charge states, $|n_0\rangle$ and $|n_0+1\rangle$, where $n_0$ is a half integer.[28,29] Take $n_0=2l+1/2$ as an example ($l=1,2,3,\ldots$), the low energy degeneracy is achieved by $(N,n_{\rm d})=(l,0)$ or $(l,1)$, where the $a$ state is either occupied or empty with a fixed Cooper pair number. Then, all terms including ${\rm e}^{\pm{\rm i}\phi}$ in $H_{\rm Md}$ can be omitted. When $n_0=2l-1/2$ by lowering an electron on the capacitor, $(N,n_{\rm d})=(l-1,1)$, $(l,0)$ are the low energy degenerate states, where the $a$ state changes accompanied by creating or eliminating a Cooper pair. In this case, only the terms $\propto{\rm e}^{\pm{\rm i}\phi}$ (the

terms raising or lowering $N$ by one) contribute to the transportation. Finally, the effective $H_{\rm Md}$ in the strong charging energy regime (note that it absorbs the effect of $H_{\rm c}$) can be rewritten as

$$H_{\rm Md} = \frac{\lambda_1}{\sqrt{2}} d_1^{\dagger} \tilde{a} - \frac{{\rm i}(-1)^n \lambda_2}{\sqrt{2}} d_2^{\dagger} \tilde{a} + {\rm h.c.}, \tag{12}$$

where $\tilde{a} = a$ when the integer $n$ is even and $\tilde{a} = {\rm e}^{-{\rm i}\phi} a^{\dagger}$ when the integer $n$ is odd. The parity of $n$ is determined by the two different resonant states, which can be changed by raising or lowering a charge.

We can replace the Nanbu representation with the basis $\Psi = (d_1, d_2, \tilde{a})^{\rm T}$, and the dimensions of all matrices can be reduced to $3 \times 3$. In this basis, the matrix form of the central system Hamiltonian and the coupling matrix can be rewritten as

$$\boldsymbol{H}_{\rm s} = \begin{bmatrix} \varepsilon_1 & 0 & \frac{\lambda_1}{\sqrt{2}} \\ 0 & \varepsilon_2 & -{\rm i}\frac{(-1)^n \lambda_2}{\sqrt{2}} \\ \frac{\lambda_1}{\sqrt{2}} & {\rm i}\frac{(-1)^n \lambda_2}{\sqrt{2}} & -\xi \end{bmatrix}, \tag{13}$$

$$\boldsymbol{\Gamma}_{\rm L/R} = \begin{bmatrix} \Gamma_1^{\rm L/R} & \Gamma_{12}^{\rm L/R} {\rm e}^{\mp \frac{{\rm i}\phi}{2}} & 0 \\ \Gamma_{12}^{\rm L/R} {\rm e}^{\pm \frac{{\rm i}\phi}{2}} & \Gamma_2^{\rm L/R} & 0 \\ 0 & 0 & 0 \end{bmatrix}. \tag{14}$$

The Fermi distribution function matrix is $\boldsymbol{F}_{\eta} = f_-^{\eta} \boldsymbol{I}_{3\times 3}$.

Since the AR is blockaded, we can apply the Landuer–Büttiker formula to transmission $T = {\rm Tr}[\,\boldsymbol{G}^{\rm a}(\omega)\boldsymbol{\Gamma}^{\rm R}\boldsymbol{G}^{\rm r}(\omega)\boldsymbol{\Gamma}^{\rm L}]$[31,32] to get charge current $I_{\rm L}$ and linear conductance $G$, where the transmission $T$ is a function of $\omega$,

$$I_{\rm L} = \int \frac{{\rm d}\omega}{2\pi} T(f_-^{\rm L} - f_-^{\rm R}), \tag{15}$$

$$G = \frac{e^2}{h} T. \tag{16}$$

## 3. Results and discussion

For numerical calculation, in both special cases, we assume $\lambda_1 = \lambda_2 = \lambda$ and equal dot levels, $\varepsilon_i = \varepsilon$ $(i = 1, 2)$. We also assume equal coupling between the $i$-th QD and the lead on the same side, i.e., $\Gamma_1^{\rm L,R} = \Gamma_2^{\rm L,R} = \Gamma_{12}^{\rm L,R} = \Gamma_{\rm L,R}$.

### 3.1. The conductance without charging energy

We assume that the nanowire is long enough so $\xi = 0$ in this subsection. In the absence of the magnetic flux ($\varphi = 0$), the three contributions to the linear conductance in Eq. (10) can be written as $T_1 = \Gamma_{\rm L}^2/y\Gamma^2$, $T_2 = \Gamma_{\rm L}\Gamma_{\rm R}/y\Gamma^2$, and $T_3 = x\Gamma_{\rm L}\Gamma_{\rm R}/\Gamma^2 y$, where $x = (1 - \omega(\omega+\varepsilon)/\lambda^2)^2 + (\omega\Gamma/\lambda^2)^2$, and $y = (1 - \omega^2/\lambda^2)^2 + (\frac{\omega(\omega^2 - \varepsilon^2 - 2\,\lambda^2 - \Gamma^2)}{2\lambda^2\Gamma})^2$. The explicit expression of the total linear conductance without charging energy is

$$G = \frac{e^2}{h}\left[\frac{2\Gamma_{\rm L}}{y\Gamma} + \frac{\Gamma_{\rm L}\Gamma_{\rm R}(x-1)}{y\Gamma^2}\right], \tag{17}$$

where $\Gamma = \Gamma_{\rm L} + \Gamma_{\rm R}$ is the full line-width function of the system.

We note that when $\omega = 0$, $x = y = 1$ and $T_1 = (\Gamma_{\rm L}/\Gamma)^2$, $T_2 = T_3 = \Gamma_{\rm L}\Gamma_{\rm R}/\Gamma^2$. The second part in the bracket of Eq. (17) will vanish, then $G_0 = G|_{\omega=0} = \frac{e^2}{h}\frac{2\Gamma_{\rm L}}{\Gamma}$. This means that the linear conductance at $\omega = 0$ is a constant and independent of the other parameters of the central system. Especially, if $\Gamma_{\rm L} = \Gamma_{\rm R}$, all transmission coefficients are $1/4$ and the total linear conductance will be fixed at $G_0 = e^2/h$. This is one of the key results in this work.

Figures 2(a) and 2(b) show the linear conductance as a function of $\omega$ for different $\lambda$ and QD levels with $\varphi = 0$. We consider the symmetrical coupling case of $\Gamma_{\rm L} = \Gamma_{\rm R}$ and assume $\varepsilon = 0$ in Fig. 2(a). As we know, in the absence of the TS nanowire and MFs ($\lambda = 0$), only the electronic tunneling process ($T_3$) contributes the conductance, and the linear conductance shows only one resonant peak at $\omega = 0$ (see the black solid line in Fig. 2(a)). As the QDs and the MBSs are coupled together ($\lambda \neq 0$), all the three contributions in the conductance expression contribute to the total conductance.[33,34] Two new resonant peaks at $\omega = \pm\sqrt{2}\lambda$ are larger than the unit conductance on account of the AR contributions.

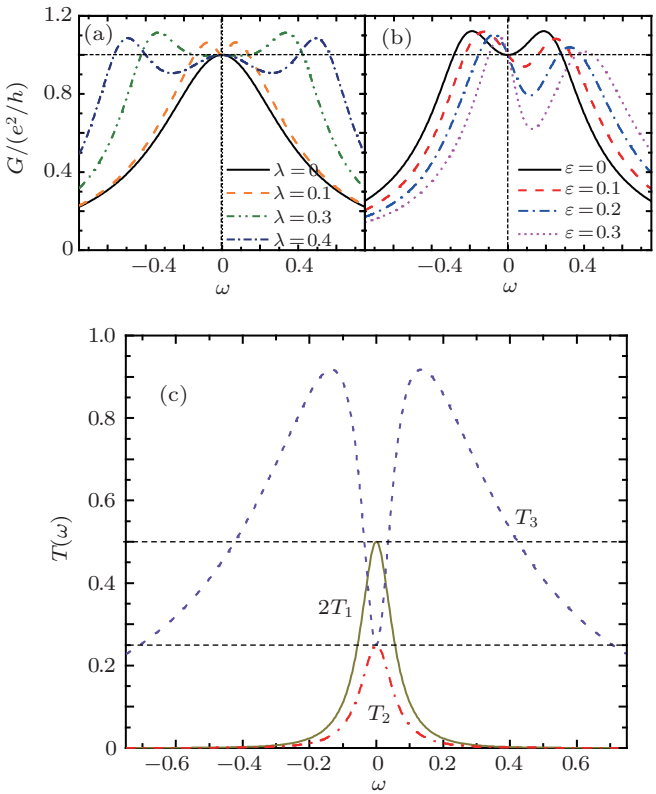



**Fig. 2.** (color online) The linear conductance as a function of $\omega$ without charging energy. (a) Fixing $\varepsilon = 0$, the black line is the conductance as a function of $\omega$ when $\lambda = 0$. Once $\lambda \neq 0$, two resonant peaks at $\pm\sqrt{2}\lambda$ are higher than $e^2/h$, companying a settled unit conductance peak. (b) Setting $\lambda = 0.2$ and tuning the levels of the QDs, the curves become asymmetrical, the resonant peaks at $\omega = (\varepsilon \pm \sqrt{\varepsilon^2 + 8\lambda^2})/2$ move, while the unit conductance at $\omega = 0$ is still fixed. (c) The details of the transmission coefficient and the AR coefficients as a function of $\omega$, where $\varepsilon = 0$ and $\lambda = 0.1$. Other parameters are $\Gamma_{\rm L} = \Gamma_{\rm R} = 0.2$ and $\xi = 0$.

The conductance at $\omega = 0$ is not affected by the properties of the QDs and MBSs. By increasing $\lambda$, the locations of two resonant peaks on the two sides are changed while the conductance at $\omega = 0$ is still fixed at the unit conductance ($G_0 = e^2/h$) (see the dashed (dot) lines in Fig. 2(a)). In Fig. 2(b), we fix $\lambda = 0.2$ and tune the QDs energy levels, the curves of conductance become asymmetrical. Meanwhile, the resonant peaks at $\omega = (\varepsilon \pm \sqrt{\varepsilon^2 + 8\lambda^2})/2$ move, while $G_0 = e^2/h$ is still localized at $\omega = 0$.

To explain this, we can regard the TS nanowire as a third terminal composed of a superconductor and two zero-mode MFs at its ends. The isolated zero-mode MFs will suppress the electronic tunneling process by anti-resonance, however the superconductivity will introduce the AR in transportation. As shown in Fig. 2(c), $T_3$ for the electronic tunneling process is partially anti-resonant and drops down to $1/4$ at $\omega = 0$ because the two QDs are coupled to the zero-mode MFs. The non-local AR coefficient $T_2$ has a peak up to $1/4$ at $\omega = 0$ because of the superconductivity of the TS nanowire. The local AR coefficient $T_1$ is doubled to $1/2$ because this AR happens at the same lead, contributing $2T_1$ to the linear conductance. Consequently, the sum of the three contributions forms the fixed unit conductance at $\omega = 0$ independent of other parameters of the central system.

### 3.2. The conductance with strong charging energy

From Eq. (12), we can see that, with the strong charging energy, when an electron tunnels from one QD through two spatially separated MBSs to the other QD, the two MBSs act as one single level system, and this process keeps the phase coherence. This Hamiltonian describes teleportation through MBSs.[28] The AR will be blockaded and $|I_L| = |I_R|$ in this situation. However, we note that there are still some differences between the MBSs in teleportation and a single level system such as a QD. The main difference between the teleportation via MBSs and that via a single level QD is reflected in the factor $\mathrm{i}(-1)^n = \mathrm{e}^{\mathrm{i}(-1)^n\pi/2}$ of Eq. (12), which is an additional phase between $d_2$ and $\gamma_2$. In order to show the differences, we calculate the conductance in the strong Coulomb regime and compare it with the result of replacing the TS nanowire by a single level QD.

In order to make the physics picture clear, it is useful to introduce the QD–molecule representation, which can make the central system be three separated single-level molecules and obtain the eigenvalues of the central system.[35] In this representation, the central system Hamiltonian and the tunneling Hamiltonian can be rewritten as

$$\tilde{H}_s = \varepsilon_0 D_0^\dagger D_0 + \varepsilon_+ D_+^\dagger D_+ + \varepsilon_- D_-^\dagger D_-, \tag{18a}$$

$$\tilde{H}_t = \sum_{k,\eta} \tilde{T}_0^\eta c_{k,\eta}^\dagger D_0 + \tilde{T}_+^\eta c_{k,\eta}^\dagger D_+ + \tilde{T}_-^\eta c_{k,\eta}^\dagger D_-, \tag{18b}$$

where $D_0$, $D_+$, and $D_-$ are the linear combinations of $d_1$, $d_2$, and $\tilde{a}$, and $\tilde{T}_{0,+,-}^\eta$ are the linear combinations of $T_{i\eta}$ ($i = 1, 2$). They are referred to the annihilation operators and the tunneling coefficients of the three decoupled and separated molecules. Now, the system has been represented as three isolated molecular states coupled with the two leads independently. The normalized occupied energy levels of the three molecules become $\varepsilon_0 = \varepsilon$ and $\varepsilon_\pm = (\varepsilon + \xi \pm \sqrt{(\varepsilon - \xi)^2 + 4\lambda^2})/2$.

According to the Landuer–Büttiker formula, the conductance expression in the strong Coulomb regime is obtained as

$$G = \frac{e^2}{h} \frac{(1 + \cos\varphi)\alpha^2}{A^2 + B^2}, \tag{19}$$

where

$$A = \frac{\alpha\Gamma - (-1)^n(\Gamma_L - \Gamma_R)\lambda^2 \sin\varphi/2}{\Gamma_L\Gamma_R},$$

$$B = \frac{(\alpha + \lambda^2)(\omega - \varepsilon)}{\Gamma_L\Gamma_R} + 2(\omega - \xi)\sin^2\frac{\varphi}{2},$$

with $\alpha = \lambda^2 - 2(\omega - \varepsilon)(\omega - \xi)$. The factor $(-1)^n$, which lies in the conductance expression, originates from the additional phase.

The conductance as a function of $\omega$ at the symmetrical case of $\Gamma_L = \Gamma_R$ is shown in Fig. 3 by setting $\varepsilon = \xi = 0$ and $\varphi = 0$. Note that there are three peaks, appearing at the locations of the three eigenvalues of the central system: $\omega = \varepsilon_0 = 0$ in the middle and $\omega = \varepsilon_\pm = \pm\lambda$ on the two sides. As we know, if the TS nanowire is replaced by a zero energy level QD, there are only two resonant peaks and one dip located at $\omega = 0$ as in the triple-QD structure (see the inset in Fig. 3). The emergence of the dip comes from the full anti-resonance when the electron energy level is near the middle QD energy level.

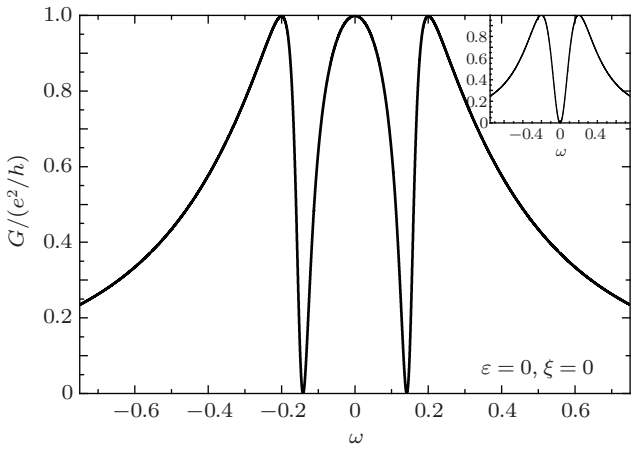



**Fig. 3.** The linear conductance as a function of $\omega$ in the strong Coulomb regime under the condition of $\Gamma_L = \Gamma_R = 0.4$. Setting $\varepsilon = \xi = 0$ and $\varphi = 0$, the peaks of linear conductance are located at $\omega = 0$ and $\omega = \pm\lambda$. The insert shows the linear conductance when the nanowire is replaced by a single level QD. The other parameter is $\lambda = 0.2$.

In our model, because of the additional phase in the teleportation Hamiltonian (Eq. (12)), the anti-resonant energy changes from $\omega = 0$ for the triple-QD structure to $\omega =$

$\pm\sqrt{2}\lambda/2$ for our structure. Consequently, the central dip in the triple-QD structure splits into two dips and a new resonant peak emerges between the two dips in our system.

The Fano effect exposes the transportation properties in an interference process, yielding an asymmetrical line shape due to the interference of transportation of a single level and a continuous channel.[36] The line-width matrix elements in the separated molecules representation read

$$\tilde{\Gamma}_{ij}^{\eta} = 2\pi \tilde{T}_i^{\eta}\, \tilde{T}_j^{\eta *} \rho_{\eta}, \quad i,j = 0,+,-. \tag{20}$$

Then the effective line widths of the three isolated molecular states can be obtained easily as

$$\tilde{\Gamma}_{00}^{\eta} = \Gamma_{\eta}\left(1+\frac{1}{2}\cos\frac{\varphi}{2}\right), \tag{21a}$$

$$\tilde{\Gamma}_{\pm\pm}^{\eta} = \frac{4\Gamma_{\eta}\lambda^2(1+\cos\varphi/2)}{4\lambda^2+A_{\pm}^2}, \tag{21b}$$

where $A_{\pm} = \sqrt{4\lambda^2+(\varepsilon-\xi)^2} \pm (\varepsilon-\xi)$. We note that the line width of the first isolated molecular state is independent of the energy levels of the two QDs and coefficient $\xi$, while the other two line widths of the states depend on the two parameters. If $\tilde{\Gamma}_{--}^{\eta}$ ($\tilde{\Gamma}_{++}^{\eta}$) increases, $\tilde{\Gamma}_{++}^{\eta}$ ($\tilde{\Gamma}_{--}^{\eta}$) just decreases conversely, and both of them are less than $\tilde{\Gamma}_{00}^{\eta}$. This gives a possibility for forming an asymmetrical line shape of the Fano resonance,[36–39] i.e., if one of them decreases to narrow enough comparing with $\tilde{\Gamma}_{00}^{\eta}$, an asymmetrical Fano resonance peak forms.

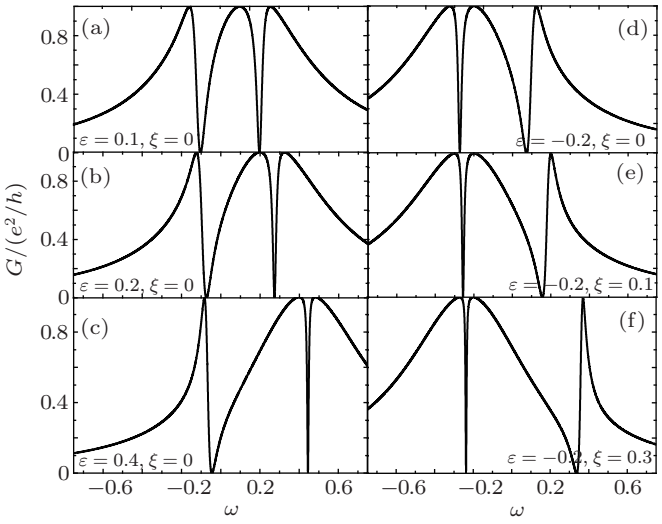



**Fig. 4.** Asymmetrical Fano resonant lines by changing the energy levels of the two QDs and the coupling amplitude of the MBSs: (a)–(c) $\varepsilon > \xi$ for fixing $\xi = 0$, the Fano line shape forms at the left side; (d)–(f) $\varepsilon < \xi$ for fixing $\varepsilon = -0.2$, the asymmetrical Fano line appears at the right side. Other parameters are $\Gamma_{\rm L} = \Gamma_{\rm R} = 0.4$ and $\lambda = 0.2$.

Figures 4(a)–4(f) show that when changing the QD levels $\varepsilon$ and $\xi$ for $\Gamma_{\rm L} = \Gamma_{\rm R}$ without the flux, two kinds of Fano lines emerge. The shape of the conductance curves depends on the value of $|\varepsilon - \xi|$, a larger value is in favor of the asymmetrical Fano line. When $\varepsilon > \xi$, say $\tilde{\Gamma}_{--}^{\eta} < \tilde{\Gamma}_{++}^{\eta} < \tilde{\Gamma}_{00}^{\eta}$, the asymmetrical line shape forms at the left side. When $\varepsilon < \xi$, say $\tilde{\Gamma}_{++}^{\eta} < \tilde{\Gamma}_{--}^{\eta} < \tilde{\Gamma}_{00}^{\eta}$, the asymmetrical line shape forms at the right side.

The formation of Fano lines can be understood easily. When the energy interval between the QDs and the MBSs is large, it is difficult to transport electrons from the up QD to the down QD through the MBSs. Meanwhile, the channels of the electron transmitting from left to right via only one QD are not affected. The direct channels can be seen as the continuous background channels, and the narrow channels crossing the two QDs via two MBSs can be seen as the discreet level channels. The interference of the two different channels produces the asymmetrical Fano line shape.

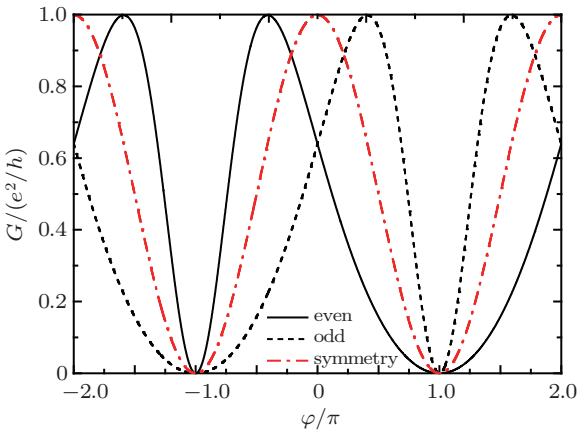



**Fig. 5.** (color online) The conductance as a function of the flux at $\omega = 0$ under the condition of left–right unequal coupling ($\Gamma_{\rm L} = 0.1$, $\Gamma_{\rm R} = 0.4$). It shows a period of $4\pi$ when the flux changes. By adding or taking off a charge on the capacitor, the parity of $n$ changes and there is a $2\pi$ phase shift due to the additional phase in teleportation. The solid black is for even $n$, while the dashed black line is for odd $n$. The red dash–dot line shows the symmetrical coupling case, $\Gamma_{\rm L} = \Gamma_{\rm R} = 0.2$, the period reduces to $2\pi$. Other parameters are $\varepsilon = \xi = 0.2$ and $\lambda = 0.2$.

More interestingly, when $\Gamma_{\rm L} \neq \Gamma_{\rm R}$, the path of electrons transmitting from the upper left arm to the lower right arm via the two QDs, interfering with the path of electrons transmitting from the left to right via only one QD (either two upper arms or two lower arms), covers only one half of the magnetic flux and generates a factor $\sin\varphi/2$. Therefore, the conductance oscillation is expected to have a period of $4\pi$. Moreover, the factor $(-1)^n$ in Eq. (19), which results from the additional phase and charging number ($n_0$) of the capacitor, will play an important role in the conductance oscillation with the magnetic flux. As shown in Fig. 5, when the parity of $n$ changes from even to odd by adding or taking off a charge on the capacitor, the transmission phase will be shifted by $2\pi$. Similar results were obtained by Fu.[28] While our results reveal that the phase shift is mainly resulted from the existence of the addition phase, and the phase shift can be tuned by QDs–leads coupling coefficients. In the symmetrical coupling case, $\Gamma_{\rm L} = \Gamma_{\rm R}$,

the factors $\sin\varphi/2$ and $(-1)^n$ in Eq. (19) vanish, therefore, the period reduces to $2\pi$ and no phase shift can be observed (the red dash–dot line shown in Fig. 5).

## 4. Summary

We have studied the transport properties of the MBSs introduced by the TS nanowire coupled to parallel QDs in an AB interferometer. We consider two special cases, the TS nanowire grounded directly and via a capacitor with strong charging energy. In the directly grounded case, we identify a conductance peak at $\omega = 0$ because the two QDs are coupled to the zero-mode Majorana, and the peak is fixed at $\omega = 0$ no matter how the QD energy level and the coupling amplitude of QDs–MBSs change. In the strong charging energy case, teleportation via MBSs will give an additional phase $\pi/2$, which is important in the path interferometer. The additional phase splits the anti-resonant dip into two dips accompanied by a resonant peak between the two dips. By tuning the energy level of the central system, two kinds of Fano line shapes can form in this strong charging energy situation. If the parity of the charging number $n$ changes, the linear conductance oscillation period with the magnetic flux will have a $2\pi$ phase shift when $\Gamma_{\rm L} \neq \Gamma_{\rm R}$. These results may provide new signatures for detecting MBSs.

## References


[1] Kitaev A Y 2001 *Physics Uspekhi* **44** 131
[2] Fu L and C L Kane 2008 *Phys. Rev. Lett.* **100** 096407
[3] Tanaka Y, Yokoyama T and Nagaosa N 2009 *Phy. Rev. Lett.* **103** 107002
[4] Beenakker C W J 2013 *Annu. Rev. Condens. Matter Phys.* **4** 113
[5] Hasan M Z and Kane C L 2010 *Rev. Mod. Phys.* **82** 3045
[6] Qi X L and Zhang S C 2011 *Rev. Mod. Phys.* **83** 1057
[7] Kitaev A Y 2003 *Ann. Phys.* **303** 2
[8] Read N and Green D 2000 *Phys. Rev. B* **61** 10267
[9] Bolech C J and Demler E 2007 *Phys. Rev. Lett.* **98** 237002
[10] Tewari S, Zhang C, Das Sarma S, Nayak C and Lee D H 2008 *Phys. Rev. Lett.* **100** 027001
[11] Moore G and Read N 1991 *Nucl. Phys. B* **360** 362
[12] Nilsson J, Akhmerov A R and Beenakker C W J 2008 *Phys. Rev. Lett.* **101** 120403
[13] Fu L and Kane C L 2009 *Phys. Rev. Lett.* **102** 216403
[14] Li X G, Zhang G F, Wu G F, Chen H, Dimitrie C and Zhang Z Y 2013 *Chin. Phys. B* **22** 097306
[15] Sau J D, Lutchyn R M, Tewari S and Das Sarma S 2010 *Phys. Rev. Lett.* **104** 040502
[16] Oreg Y, Refael G and von Oppen F 2010 *Phys. Rev. Lett.* **105** 177002
[17] Alicea J 2010 *Phys. Rev. B* **81** 125318
[18] Ivanov D A 2001 *Phys. Rev. Lett.* **86** 268
[19] He K, Ma X C, Chen X, Lü L, Wang Y Y and Xue Q K 2013 *Chin. Phys. B* **22** 067305
[20] Yuan J H, Cheng Z, Zhang J J, Zeng Q J and Zhang J P 2012 *Chin. Phys. B* **21** 047203
[21] Liu Y, Ma Z, Zhao Y F, Meenakshi S and Wang J 2013 *Chin. Phys. B* **22** 067302
[22] Flensberg K 2010 *Phys. Rev. B* **82** 180516
[23] Mourik V, Zuo K, Frolov S M, Plissard S R, Bakkers E P A M and Kouwenhoven L P 2012 *Science* **336** 1003
[24] Rokhinson L P, Liu X Y and Furdyna J K 2012 *Nat. Phys.* **8** 795
[25] Das A, Ronen Y, Most Y, Oreg Y, Herblum M and Shtrikman H 2012 *Nat. Phys.* **8** 887
[26] Deng M T, Yu C L, Huang G Y, Larsson M, Caroff P and Xu H Q 2012 *Nano Lett.* **12** 6414
[27] Liu J, Potter A C, Law K T and Lee P A 2012 *Phys. Rev. Lett.* **109** 267002
[28] Fu L 2010 *Phys. Rev. Lett.* **104** 056402
[29] Zazunov A, Yeyati A L and Egger R 2011 *Phys. Rev. B* **84** 165440
[30] Hützen R, Zazunov A, Braunecker B, Yeyati A L and Egger R 2012 *Phys. Rev. Lett.* **109** 166403
[31] Liu D E and Baranger H U 2011 *Phys. Rev. B* **84** 201308
[32] Datta S 1995 *Electronic Transport in Mesoscopic Systems* (1st edn.) (London: Cambridge University Press)
[33] Meir Y and Wingreen N S 1992 *Phys. Rev. Lett.* **68** 2512
[34] Lü H F, Lu H Z and Shen S Q 2012 *Phys. Rev. B* **86** 075318
[35] Cao Y, Wang P, Xiong G, Gong M and Li X 2012 *Phys. Rev. B* **86** 115311
[36] Zhu B F, Lu H and Lü R 2005 *Phys. Rev. B* **71** 235320
[37] Fano U 1961 *Phys. Rev.* **124** 1866
[38] Kobayashi K, Aikawa H, and Katsumoto S and Iye Y 2002 *Phys. Rev. Lett.* **88** 256806
[39] Göres J, Goldhaber-Gordon D, Granger G, Kastner M A, Shtrikman H, Mahalu D and Meirav U 2000 *Phys. Rev. B* **62** 2188